On the origin of the electrostatic potential difference at a liquid-vacuum interface

Edward Harder and Benoît Roux[a)]
Department of Biochemistry and Molecular Biology, Center for Integrative Science, University of Chicago, Chicago, Illinois 60637, USA

(Received 19 August 2008; accepted 23 October 2008; published online 17 December 2008)

The microscopic origin of the interface potential calculated from computer simulations is elucidated by considering a simple model of molecules near an interface. The model posits that molecules are isotropically oriented and their charge density is Gaussian distributed. Molecules that have a charge density that is more negative toward their interior tend to give rise to a negative interface potential relative to the gaseous phase, while charge densities more positive toward their interior give rise to a positive interface potential. The interface potential for the model is compared to the interface potential computed from molecular dynamics simulations of the nonpolar vacuum-methane system and the polar vacuum-water interface system. The computed vacuum-methane interface potential from a molecular dynamics simulation (−220 mV) is captured with quantitative precision by the model. For the vacuum-water interface system, the model predicts a potential of −400 mV compared to −510 mV, calculated from a molecular dynamics simulation. The physical implications of this isotropic contribution to the interface potential is examined using the example of ion solvation in liquid methane. © *2008 American Institute of Physics*.
[DOI: 10.1063/1.3027513]

I. INTRODUCTION

A distinct structural asymmetry characterizes spatial regions that lie at the interface between media. This asymmetry can give rise to an imbalance of charge that produces a difference in the electrostatic potential across the interface. Such potentials arise at the interface between hydrating water and proteins or phospholipid membranes and their role has been cited in the structure and function of membrane bound proteins[1–5] and the differential conductance of negative versus positively charged species across the bilayer.[6–8] Far less complex are interface regions that separate two isotropic bulk media, although similar interface potentials have also been observed across liquid-liquid and liquid-vacuum interfaces.[9,10] One example of particular importance in areas of atmospheric chemistry[11–13] is the vacuum-water interface. In part, due to the inherent difficulties associated with measuring absolute interface potential, the nature of this observable for both complex and simple systems alike remains poorly understood. For example, estimates for the vacuum-water interface potential disagree considerably in value and even sign.[9]

In the absence of robust experimental measurements, results from computer simulations based on detailed atomic models can be used to provide insight on this issue. The average electrostatic potential drop across a liquid-vacuum interface can readily be calculated from the average atomic charge distributions generated from computer simulations. Remarkably, molecular simulations have been shown to consistently predict a significant voltage drop across a liquid-vacuum interface. For the water-vacuum system, simulations based on a variety of atomic potential functions (some accounting for induced polarization) have consistently estimated the interface potential to be ≈−500 mV.[14]

The underlying physical determinant of the vacuum-water interface potential is often ascribed to the particular orientation of surface water molecules.[9,15–17] However, attempts to characterize the interface potential based solely on the orientational correlation of molecules have lead to qualitatively erroneous predictions.[18,19] Missing from such an analysis is an appropriate account for the contribution to the interface potential from the molecular quadrupole.[19] A consequence of this consideration is that even isotropically oriented molecules will contribute to the interface potential. In fact, there is evidence that nondipolar contributions may be considerable. Recently, Patel and Brooks[20] computed an interface potential of −400 mV from a molecular simulation of the vacuum-hexane interface. Somewhat surprisingly, the magnitude and sign of the interface potential for this nonpolar system is roughly of the same order of magnitude to that computed from simulations of the vacuum-water interface.

The consistent observation of such large potential differences across liquid-vacuum interfaces in polar and nonpolar systems alike, from simulations based on a variety of atomic models, simply cannot be explained by the orientational ordering of dipoles alone. This puzzling result led us to examine the consequences of an exceedingly simple model of the interface potential. The model, by construction, has no orientational order of the molecules neither in the bulk nor at the interface. Nevertheless, average electrostatic potentials are built into this simple model, which may be considered as a convenient zeroth-order isotropic reference system of the

[a)]Author to whom correspondence should be addressed. Electronic mail: roux@uchicago.edu.

liquid. In the following, we show that such a simple model yields interface potentials of the same sign and similar magnitude to those computed from molecular dynamics (MD) simulations of fully atomistic force field models. This agreement points to a fundamental relationship between the interface potential and the spatial structure of the charge distribution within a single molecule. We examine the implications of this result and use the model to comment on the role of such interface potentials in the solvation of charged species. It is worth noting that the results of the conceptual model studied herein are closely related to the isotropic contribution derived as part of the pioneering work of Wilson *et al.*[19] and later used to illustrate the effects of force truncation in the calculation of electrostatic forces for molecular simulation.[21,22]

Details of the MD simulations used in this report are summarized in Sec. II. In Sec. III the interface potential model (IP Model) is developed. Section IV discusses general features of the model, compares the predicted interface potential to MD simulations of the vacuum-methane and vacuum-water systems and briefly discusses the impact on molecule solvation. Concluding remarks are summarized in Sec. V.

II. SIMULATION DETAILS

All MD simulations are performed with the program CHARMM (Ref. 23) using a velocity Verlet algorithm[24] with a 2 fs time step. The temperature in the neat liquid and interface simulations is controlled by a Nose–Hoover thermostat.[25] In the constant pressure equilibration the pressure is controlled by an Andersen–Hoover barostat.[26] Periodic boundary conditions were used in all liquid simulations. A particle mesh approximation to the Ewald sum with "tin foil" boundary conditions is used to evaluate the Coulombic interactions in the liquid simulations.[27] A smooth real space cutoff is applied between 10–12 Å an Ewald splitting parameter of 0.34 $Å^{-1}$ a grid spacing of ≈ 1.0 Å and a sixth order interpolation of the charge to the grid is used. The same cutoff scheme is used for the Lennard-Jones (LJ) potential. The SHAKE/Roll and RATTLE/Roll procedure[28,29] are used to constrain covalent bonds to hydrogens.

Simulations of water are performed with the TIP3P (Ref. 30) force field. Parameters used in simulations of the methane force field model are consistent with CHARMM (Ref. 31) and include minor modifications made to account for the tetrahedral symmetry of the molecule.

A neat liquid cubic unit cell of 500 water and 500 methane molecules is equilibrated for 100 ps in the NPT ensemble at a pressure of 1 atm and temperatures of 298 and 100 K for the water and methane simulations, respectively. The coordinates and unit cell corresponding to the final step in this equilibration is used as initial conditions for simulations of the neat liquid and interfacial systems run in the NVT ensemble. A protocol is adopted for building vacuum-liquid-vacuum systems that is similar to previous work.[17,20,32] One dimension of the unit cell is extended to build a vacuum-liquid-vacuum system that is equilibrated for a further 100 ps. Statistics are collected for 5 ns of simulation time for the vacuum-water interface system and the neat liquid water simulation. Statistics are collected for 500 ps for the vacuum-methane interface system.

The solvation-free energy of a LJ sodiumlike ion[31] in liquid methane is computed using thermodynamic integration.[33] Positively and negatively charged ions are examined with the same radius. Simulations consist of the sodiumlike ion solvated by 250 methane molecules at the density corresponding to the bulk liquid phase of the methane liquid-vacuum simulation. The integration was partitioned into ten windows with statistics averaged over 100 ps of simulation time. The free energy is computed at 100 K in two geometries: a spherical liquid drop and under periodic boundary conditions.

III. THE IP MODEL

Let us consider an electrostatic model of an atom that consists of a localized positive charge at the atom center (nuclei) and a surrounding Gaussian distributed negative charge (electrons). The charge distribution of the atom is

$$\rho(r) = Z\left(\delta(r) - \frac{e^{-r^2/2\sigma^2}}{(2\pi)^{3/2}\sigma^3}\right), \tag{1}$$

where Z is the charge of the nuclei. To extend this model to molecules we consider the charge distribution of a collection of atoms. In a coordinate frame where the origin corresponds to the geometric center of the molecule the radial charge distribution is

$$\rho(r) = \sum_i Z_i\left(\delta(r - r_i) - \frac{e^{-(r-r_i)^2/2\sigma_i^2}}{C_i}\right). \tag{2}$$

In real molecules the electronic charge distribution does not remain centered about the constituent nuclei, rather, more electronegative atoms attract charge away from less electronegative atoms. In our model we presume a negative electronic charge Q shifts from a point located at R_2 from the atom center to a point R_1. The result is an excess of electronic charge at R_1 and a depletion of charge at R_2. The radial charge distribution then becomes

$$\rho(r) = \sum_i Z_i\left(\delta(r - r_i) - \frac{e^{-(r-r_i)^2/2\sigma_i^2}}{C_i}\right) + Q\left(\frac{e^{-(r-R_1)^2/2\sigma^2}}{C_-} - \frac{e^{-(r-R_2)^2/2\sigma^2}}{C_+}\right). \tag{3}$$

The charge density associated with the first term is representative of a system of noninteracting neutral atoms. Qualitatively, the second term aims to capture the perturbation of this reference charge system as atomic charge densities form molecules.

An interface potential arises when there is an excess of charge along the coordinate normal to the interface. Assuming that the molecules are isotropically oriented, we integrate over the orientational degrees of freedom. The charge density along the interface normal (z) for the model centered at the origin is

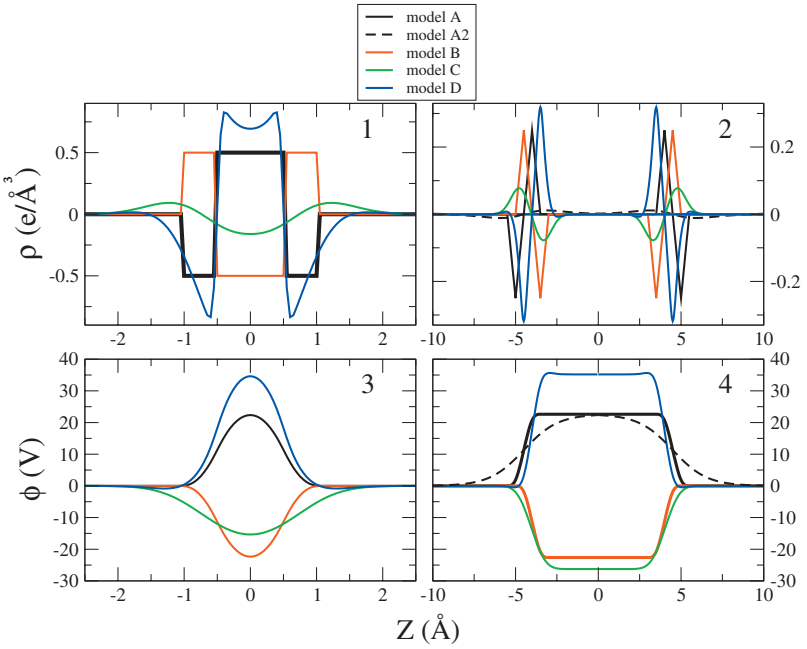

FIG. 1. (Color) The charge density and potential for five parametrical variations of the IP model. The parameters for the five models are given in Table I. The left panels show the charge density and potential for the models with center fixed at the origin (the black solid and dashed lines are identical in these panels). The right panels show the charge density and potential for an interfacial system with boundaries at $L=\pm 5$ Å. For point charge models the potential is positive for models with R_1 greater than R_2 and negative for models with R_2 greater. Models C and D have Gaussian distributed radial charge distributions with finite width σ. Model D includes a contribution that corresponds to the neutral atom potential. Models A, A2, and B correspond to the point charge limit (i.e., $\sigma=0$). The molecule density of the monomer is set to $1(\mathrm{N/Å^3})$. For models A, B, C and D the molecule density (ρ_{z_c}) is a step function equal to $1(\mathrm{N/Å^3})$ between the boundaries and zero otherwise. The interface width characterized by the change in ρ_{z_c} is finite (≈ 4 Å) for model A2.

$$\rho(z) = \sum_i Z_i(\Theta(r_i - |z|)/2r_i - P_i(z)) + Q(P_-(z) - P_+(z)), \tag{4}$$

where the probability of finding the positive point charge is given by a Heavyside function $\Theta(r_i - |z|)$ and the $P(z)$ functions are the probabilities of finding charge along z associated with each of the Gaussians in Eq. (3). Taking the probability associated with the Gaussian of particle i as an example,

$$P_i(z,z_c) = \frac{2\pi\left(\sigma_i^2 e^{-(r_i-|z-z_c|)^2/2\sigma_i^2} + \sigma_i r_i\sqrt{\frac{\pi}{2}}\left(1+\mathrm{erf}\left(\frac{r_i-|z-z_c|)}{\sqrt{2}\sigma_i}\right)\right)\right)}{C_i}, \tag{5}$$

where C_i is a normalization constant (see Appendix for details). To get the charge density for an interfacial system we need to integrate over translations of z_c. For a molecule density, ρ_{z_c}:

$$P_i(z) = \frac{\int_{-\infty}^{\infty} P_i(z,z_c)\rho_{z_c} dz_c}{C_L}, \tag{6}$$

where C_L is the normalization constant. The hyperbolic tangent function has been shown to fit well to molecular density profiles determined from MD simulations:[34]

$$\rho_{z_c} = \tfrac{1}{2}\rho_0[1 + \tanh(K_w(L - |z|))], \tag{7}$$

where ρ_0 is the density in the bulk region and K_w is a parameter that modulates the width of the interface region. In the limit that $K_w \to \infty$ the molecular density reduces to a step function with $\rho_{z_c}=\rho_0$ for $|z|<L$ and zero otherwise. Finally, the electrostatic potential along the interface normal can be computed from the charge density profile, as a solution to the Poisson equation $\partial^2\phi(z)/\partial z^2 = -4\pi\rho(z)$:

$$\phi(z) = -2\pi\int_{-\infty}^{z} dz'\left[\int_{-\infty}^{z'} dz''\rho(z'') - \int_{z''}^{\infty} dz''\rho(z'')\right]. \tag{8}$$

The interfacial potential defined by Eq. (8) corresponds to the standard internal Galvani potential. This potential cannot be measured experimentally by any physical process (though it can be defined mathematically without ambiguity as shown here).

IV. RESULTS AND DISCUSSION

A. The IP model

For a given charge Q and atomic charges Z_i the interface potential model is distinguished by two features. The relative distance $R1$ to $R2$ and the widths (σ_i and σ) associated with the radial charge distribution. Interface potential corresponding to various IP models are plotted in Fig. 1. Corresponding parameters are summarized in Table I.

TABLE I. Parameters for the IP models.

Name	σ_1 (Å)	Z_1 (e)	σ (Å)	Q (e)	R_1 (Å)	R_2 (Å)
Model A/A2	0	2	0	−1.0	1.0	0.5
Model B	0	2	0	−1.0	0.5	1.0
Model C	0	2	0.5	−1.0	0.5	1.0
Model D	0.5	2	0.5	−1.0	0.5	1.0

The effect of, $\Delta R = R_2 - R_1$, on the interface potential is illustrated by the point charge IP models, A/A2 and B. In the point charge regime of the interface potential model, the charge density associated with the atomic charges Z_i is rigorously zero everywhere. In models A and A2 the relative distance, ΔR, is negative. In model B, ΔR is positive. Given the convention used in Sec. III to develop the IP model, a relative distance that is negative will correspond to a negative charge density near the surface of the molecule and a positive charge density closer to the molecular center. When ΔR is positive, the charge density is negative closer to the interior of the molecule. This behavior is illustrated in panel 1 of Fig. 1, which shows the one dimensional projection of the model molecule charge density. The corresponding interfacial charge density and potentials are plotted in panels 2 and 4, respectively, of Fig. 1. For IP model, where ΔR is positive, the interface potential is negative while a negative ΔR gives a positive interface potential. Thus, according to the IP model, molecular charge densities that are point-charge-like and have more electronegative atoms toward their interior will tend to give interface potential that are negative. This observation would appear to encompass the rather broad set of organic molecules composed of carbon, nitrogen, and oxygen atoms surrounded by hydrogens and qualitatively explains the negative interface potential calculated from molecular simulations of water[14] and nonpolar hexane.[20] When ΔR is negative, the point-charge-like IP model predicts an interface potential that is positive. This is akin to a molecule that has more electronegative nuclei at its periphery. This would include organic molecules where hydrogen atoms are replaced by halogen atoms.

Unlike the charge density of point charge based force fields, real molecules are characterized by smoothly varying electron densities. In the IP models these smoothly varying charge densities are given a Gaussian form. The impact on the interface potential is examined by comparing two analogs of the previously discussed model B. For simplicity, we consider the model to consist of only one nonzero atomic charge Z_1 at the position R_1. The charges Q and Z_1 and the relative distance (ΔR) are the same for models B and C. The radial charge density of Q and Z_1 in model B is point charge like. In model C, Q has a finite width and Z_1 is point-charge-like. As a consequence, the first term of Eq. (3) vanishes for both models B and C. Qualitatively the behavior of models B and C is similar with the potential becoming more negative when the molecule charge density Q is made smooth.

This qualitative picture, where the sign of the interface potential is simply related to the sign of ΔR, changes dramatically when one considers IP models with a finite width for the neutral atom charge density, Z_1. As in models B/C, ΔR is positive for model D. Unlike the latter two models, model D has a smooth negative charge density associated with Z_1. For the parametrical assignments made to model D, this additional atomic potential contribution to the charge density has the effect of changing the behavior of the molecule charge density (see panel 1 in Fig. 1). In models B/C the molecule charge density is more positive at the periphery of the molecule while in model D it is more negative. As a consequence the interface potential shown in panel 4 of Fig. 1 changes from negative in B/C to positive in model D.

Fundamentally, the interface potential computed for all the IP models is related to the sign of the charge density at the molecule surface relative to its core. This basic relationship for isotropically oriented molecules has been recognized previously. In an early study of the interface potential of water, Wilson *et al.*,[19] showed that the isotropic contribution to the interface potential is related to the trace of the quadrupole tensor. The isotropic contribution to the potential difference between an isotropic bulk liquid and vacuum is

$$\phi_{\mathrm{iso}} = -\frac{4\pi}{6}\sum_j q_j r_j^2(\rho_{\mathrm{bulk}} - \rho_{\mathrm{vac}}), \tag{9}$$

where r is taken with respect to a chosen molecular center and ρ_{bulk} and ρ_{vac} are the average molecule density in the bulk and vacuum phase, respectively. Indeed, computing the potential from this quadrupole term gives equivalent results to the potential difference observed in our IP model.

According to Gauss's law[35] the difference in the interface potential between the center of the bulk and the vacuum will be invariant to the shape of the molecular charge distribution in the interface region. This is shown in the comparison of models A and A2 shown in Fig. 1. The models are differentiated solely by the choice of ρ_{z_c}. For model A the molecule density is a step function and for model A2 the density varies smoothly between the vacuum and bulk. This has a dramatic affect on the charge density as shown in panel 1 of Fig. 1 but the potential difference remains unchanged. For simplicity, further applications of the IP model will use a molecule density that corresponds to a step function.

B. Applications

The central assumption of the IP model is that molecules are isotropically oriented with respect to the laboratory frame. As such, the model does not capture the microscopic orientational ordering that arises from intermolecule associations. Such ordering is averaged away in the ensemble of configurations that constitute a bulk liquid environment and the approximation is exact in this regime. In general, this is not the case near an interface boundary. Wilson *et al.*,[19] have shown that a precise assessment of the interface potential should also include an orientation dependent term

$$\phi_{l\to v} = \phi_{\mathrm{iso}}(c) + \phi_{\mathrm{orient}}(c), \tag{10}$$

where ϕ_{iso} is akin to the potential difference of the IP model and ϕ_{orient} depends on the orientational correlation of molecular dipoles. The relative weights of the isotropic and orientation terms are controlled by a parameter (c) which corresponds to the choice of molecule center in the molecular reference frame of the IP model. In the IP model we consider a conceptual partition of these two contributions where c corresponds to the geometric center of the molecule and ϕ_{iso} is thus analogous to a liquid system of close packed hard spheres with embedded charges. In the following sections we examine the relationship between the interface potential of a fully atomistic detailed MD simulations of vacuum-methane and vacuum-water interface systems and ϕ_{iso}.

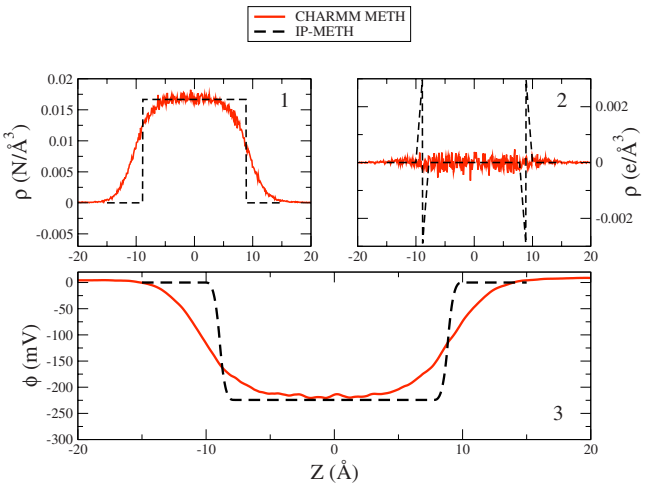

FIG. 2. (Color online) Shown are the molecule density, charge density, and potential along the interface normal of the vacuum-methane system. The molecule density is plotted in the top left panel, the charge density is plotted in the top right panel and the interface potential is plotted in the bottom panel. The data for the CHARMM-METH model correspond to a simulation, using the CHARMM force field, of a liquid methane slab comprised of 500 molecules surrounded by vacuum. The IP-METH model is the simple model of methane with parameters translated from the CHARMM model of methane.

1. Vacuum-methane interface

As a more realistic representation of a vacuum-liquid interface, 500 methane molecules forming a liquid slab bordered by vacuum are simulated using the CHARMM force field.[31] The molecule density along the interface normal is plotted in panel 1 of Fig. 2. The broad interface region, extending over nearly 10 Å, gives rise to a gradual drop in the electrostatic potential from vacuum to the bulk. The potential at the center of the liquid methane region is −220 mV relative to the vacuum.

Choosing parameters for the IP model of methane (IP-METH) that correspond to the force field model of methane is straightforward. The electrostatic parameters of the CHARMM force field consists of a negative point charge at the position of the carbon atom and positive point charges that are positioned on the hydrogen atoms. Taking the molecule center to coincide with the position of the carbon atom, the parameter $R1$ is zero and the parameter $R2$ corresponds to the distance of the carbon-hydrogen bond. The charge Q is the charge of the carbon atom and both σ and σ_i are equal to zero for a point charge model. A summary of the parameters for the IP-METH model is given in Table II. The molecule density at the center of the bulk region is set to correspond to the measured bulk density from the CHARMM simulation. The interface region of the IP model corresponds to a discrete drop in the molecule density from this bulk value to zero. As a consequence, changes in the charge density occur on the length scale of a single molecule. Nevertheless, the total potential drop of the IP model is 220 mV, in excellent agreement with the value measured from the simulation.

2. Vacuum-water interface

The IP model for water is based on the TIP3P force field.[30] The TIP3P force field consists of a negative point charge on the position of the oxygen atom and positive point charges at the hydrogen positions. The charge Q is the charge of the oxygen atom and since this is a point charge model, σ and σ_i are equal to zero. The parameters R_1 and R_2 will depend on an appropriate choice for the molecule center. Unlike the IP model of methane there is some ambiguity in choosing the molecule center for a polar molecule.

To illustrate the sensitivity of the IP water model to different choices of molecular center, three IP-TIP3P models of water are investigated. Model IP-TIP3a assigns the model center to the position of the oxygen atom. The center of the IP-TIP3b model is the geometric center of TIP3P and the IP-TIP3c center is on the molecule bisector at the point closest the hydrogen atoms. The interface potential are shown in Fig. 3. For all three models, ΔR is positive making the interface potential negative in the bulk phase relative to the vacuum. The difference between R_1 and R_2 is smallest when the center is closest the hydrogen atoms and largest when the center is coincident with the oxygen. This is reflected in the relative magnitude of the potential drop for each model.

Isomorphic vacuum-water interface system can be built from MD simulations of the TIP3P force field. A neat liquid water simulation consisting of 500 TIP3P water molecules under periodic boundary conditions is generated. In this system, the water molecule orientations are on average isotropic everywhere. The atomic coordinates generated from this simulation are then postprocessed to build a virtual vacuum-water interface. Molecules in the reference unit cell are used as the bulk phase and coordinates for image molecules are removed, forming the surrounding vacuum phase. For molecules that overlap with the boundary between the bulk and vacuum phases the periodic boundary condition is applied in a consistent manner with the choice of molecular center used in the IP models. For example, in accord with the choice of center in the IP-TIP3a model, water molecules or their periodic image are considered part of the bulk phase based on the position of the oxygen atom with respect to the unit cell boundary. If the oxygen atom lies outside the unit cell, the

TABLE II. Parameters for the IP models of methane and water. The IP-TIP3Pb* model includes a nonvanishing atomic potential with charge $Z_1=8e$ and a width $\sigma_1=0.5$ Å. All other models are point charge based.

Molecule	Name	σ (Å)	Q (e)	R_1 (Å)	R_2 (Å)
Methane	IP-METH	0	−0.36	0	1.111
Water	IP-TIP3Pa	0	−0.834	0	0.9572
Water	IP-TIP3Pb	0	−0.834	0.39	0.49
Water	IP-TiP3Pc	0	−0.834	0.585	0.757
Water	IP-TIP3Pb*	0	−0.834	0.39	0.49

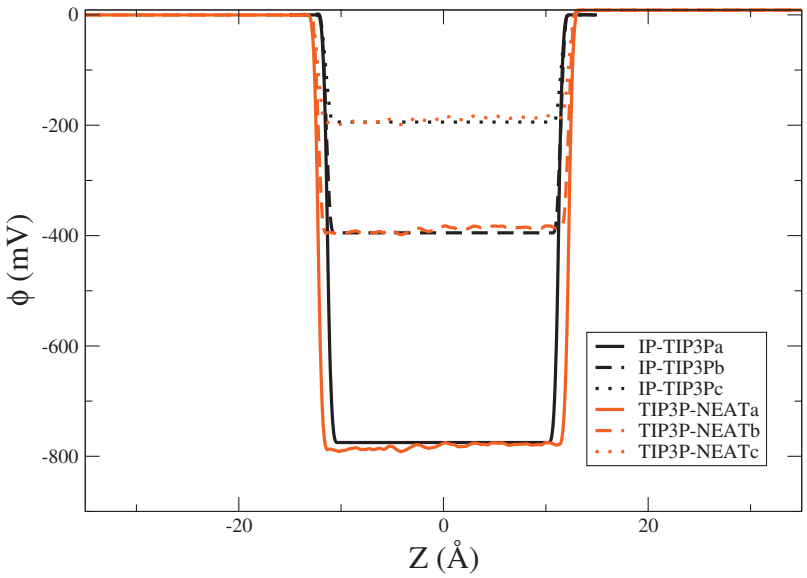

FIG. 3. (Color) The potential drop along the interface normal for three IP models of the TIP3P water force field. The center of the IP-TIP3Pa corresponds to the position of the oxygen atom. The center of the IP-TIP3Pb model is the geometric center of the molecule and the center of the IP-TIP3Pc model is along the H–O–H bisector closest to the hydrogen atoms. The potential in the bulk region of the interface model is negative with respect to the vacuum for all three models. Also included are the interfacial potential computed from simulation of neat liquid water in PBCs with the TIP3P force field. Image atoms are replaced by vacuum leaving only the molecules of the reference unit cell. Boundary conditions are applied to positions on the molecule that are analogous to the choice for molecular center in the IP models.

position of the oxygen atom for its periodic image will lie within the unit cell and this image is thus chosen as part of the bulk phase. The resultant potential from this neat liquid simulation is labeled TIP3P-NEATa. Similarly, the assignment of boundary waters or their image to the bulk phase can be made based on the geometric center (TIP3P-NEATb) or the bisector point closest to the hydrogen atoms (TIP3P-NEATc) as in the center assignment in the IP-TIP3b and IP-TIP3c models, respectively. The corresponding interface potentials are plotted in Fig. 3. The potentials from these simulations correspond perfectly to their analogs in the IP models.

To compare with a more realistic simulation of a vacuum-water interface, the IP model whose center coincides with the geometric center of the TIP3P force field (i.e., IP-TIP3Pb) is chosen. This choice is based on the simple rational that molecules at the interface prefer to be solvated by surrounding molecules and will therefore tend to minimize their exposed surface area to vacuum. The realistic vacuum-water interface system is generated from a MD simulation of 500 TIP3P water molecules forming a liquid slab surrounded by vacuum. The molecule and charge density from the simulation and IP-TIP3b model are presented in the top panels of Fig. 4. Panel 3 shows the corresponding potential profile. The potential drop for IP-TIP3Pb is 400 mV, in reasonable agreement with the MD simulation value of 520 mV.

It is clear from Fig. 3 that varying the center of the IP model between the geometric center and the oxygen atom position can lead to precise agreement with the interface potential calculated from the MD simulation. However, this does not imply that the orientational structure of water molecules at a vacuum-water interface system is purely isotropic, as it is assumed by construction in the IP model. Experiments have shown that water molecules adopt a subtle orientational order in the interface region between the liquid and vacuum.[36] This orientational structure does not go away with an appropriate choice of molecular center but the cumulative contribution to the IP does go to zero.

Missing from these atomistic force fields of water and methane are atomic charge densities, Z_i. This core atom electron density has a benign affect on the intermolecule electrostatic interactions between molecules and are justifiably excluded from the electrostatic description of these force field models. However, the inclusion of this contribution can have a dramatic affect on the interface potential (see Sec. IV A). Taking water as an example, we consider the IP-TIP3Pb model with the addition of an atomic potential that is reasonably consistent with the atomic properties of an oxygen atom (IP-TIP3Pb*). The atom potential is centered on the oxygen atom (R_1) with a charge of $Z_1=8e$ and a negative charge density width that is $\sigma_1=0.5$ Å. The resultant potential, shown in panel 4 of Fig. 4, is approximately 7 V. This is nearly an order of magnitude larger in magnitude and of opposite sign to the potentials calculated from the IP-TIP3P model or the associated TIP3P force field. Such a large posi-

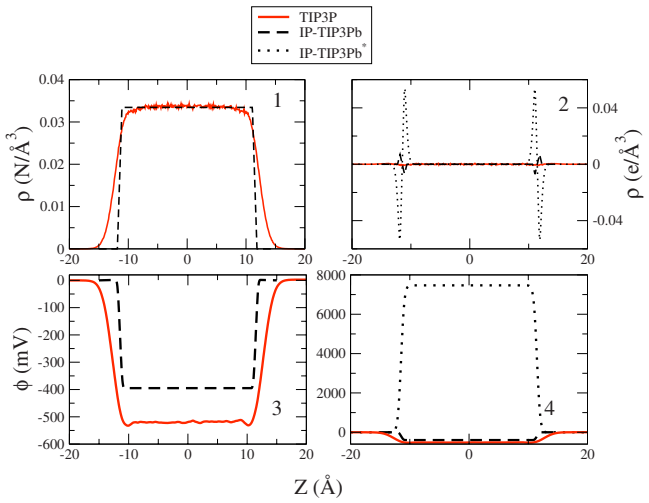

FIG. 4. (Color online) Shown are the molecule density, charge density, and potential along the interface normal of the vacuum-water system. The molecule density is plotted in the top left panel, the charge density is plotted in the top right panel and the interface potential is plotted in the bottom panel. The data for the TIP3P model are from a simulation of a liquid water slab comprised of 500 molecules surrounded by vacuum. The IP-TIP3Pb model is the IP model translated from the TIP3P water force field with molecular center chosen to coincide with the geometric center of the molecule. The IP-TIP3Pb* model includes an atomic potential contribution.

tive interface potential was also observed at the vacuum-liquid interface for a force field simulation of water with quantum mechanical-like charge densities.[37] The sensitivity of the interface potential to features of the molecular charge distribution that are not expected to effect intermolecule interactions is surprising. This seemingly paradoxical observation is clarified in the following discussion.

C. Interface potential and the solvation energy

The solvation-free energy of a charge q embedded in a solute sphere of radius R and surrounded by a dielectric continuum (ϵ) is given by the Born energy:[38]

$$\Delta G_{\mathrm{Born}} = \frac{-q^2}{2R}(1 - 1/\epsilon). \tag{11}$$

This equation assumes that the charged ion is immersed in an infinite bulk region. Contributions to the solvation energy that depend on the interface potential are absent from Eq. (11). In this report we have considered the macroscopic interface potential ($\phi_{\mathrm{l}\to\mathrm{v}}$) due to the bulk liquid-vacuum interface. Additionally, one might imagine that there is also a microscopic potential (ϕ_{micro}) due to the interface between the solute and the solvent. Recent studies have measured a nonzero potential within an uncharged LJ solute due to the surrounding solvent.[39–41] This is the solute-solvent interface potential. Including these contributions into the solvation free energy, yields

$$\Delta G_{\mathrm{real}} = q(\phi_{\mathrm{micro}} + \phi_{l\to v}) - \frac{q^2}{2R}(1 - 1/\epsilon). \tag{12}$$

where the label "real" is used for consistency with previous work.[14] One may also wish to consider the solvation-free energy that is independent of the bulk liquid-vacuum interface potential. This "intrinsic" solvation free energy is

$$\Delta G_{\mathrm{intr}} = \Delta G_{\mathrm{real}} - q\phi_{l\to v}. \tag{13}$$

In the IP model there is no distinction between a vacuum-liquid interface and a solute-liquid interface. In this model, the potential due to the bulk liquid-vacuum interface is of equal magnitude and opposite sign to the potential due to the solute-liquid interface and the solvation expressed by ΔG_{real} will be independent of any isotropic contributions to the interface potential. By contrast, ΔG_{intr} is functionally dependent on the interface potential ϕ_{micro} and contributions to this potential from isotropic moments of the molecular charge density. According to Gauss's law,[35] embedding an arbitrary spherically symmetric charge distribution within the excluded volume of the solute will not affect intermolecule interactions and will therefore not affect simulated particle trajectories or the resultant solvation-free energy. However, such a charge distribution will affect the interface potential and thus ΔG_{intr}. More broadly, the issues concerning the solvation of ions discussed here are also related to the familiar P-sum (particle-based) and M-sum (molecule-based) conventions introduced to offset the value of the electrostatic potential in periodic systems treated with Ewald lattice sum approaches. With both conventions the computed intrinsic free energies ΔG_{intr} of charged ions in periodic systems leave out the contribution from the interface potential, $q\phi_{l\to v}$, the magnitude of which depends on whether a P-sum or M-sum convention has been utilized.[42] In the P-sum convention the missing interface potential $\phi_{l\to v}$ is given by Eq. (8). In the M-sum convention the electrostatic potential is shifted by a constant associated with the isotropic quadrupole contribution given in Eq. (9), which depends on the arbitrarily chosen position for the center of the molecule. In either case, the intrinsic free energy reflects the arbitrary convention used to define the interfacial Galvani potential, a quantity that is not actually measurable physically.[43] This ambiguity is untenable and the physically relevant expression for ion solvation to consider is ΔG_{real}. This consideration further clarifies the benign role of the atomic charge density of water that nonetheless leads to a dramatic 7 V interface potential (see Sec. IV B 2). Because the atomic potential is part of the isotropic moment of the molecular charge density, the very large individual miscroscopic and macroscopic interface potential will cancel leaving little contribution to the physically relevant solvation of a charged species.

TABLE III. The solvation-free enegy difference between monovalent sodium and a negatively charged analog in liquid methane. The free energy is computed for two systems: a sodiumlike ion solvated in the center of a spherical liquid drop and under periodic boundary conditions (PBCs). PBC* includes a correction for the missing liquid to vacuum interface potential (i.e., $q\phi_{l\to v}$) where $\phi_{l\to v}$ from the methane-vacuum simulation is −220 mV and q is $-2e$ to change a $+1e$ sodiumlike ion to $-1e$.

Geometry	$\Delta G_{+\to -}$ (kcal/mol)
Sphere	0.3 ± 0.5
PBC	-9.6 ± 0.5
PBC*	0.4 ± 0.5

The example of ion solvation in liquid methane is illustrative. The molecular charge density of methane consists predominantly of an isotropic quadrupole moment. According to the preceding discussion, even though the liquid-vacuum interface potential of methane is quite large (−220 mV) the solvation of ions in bulk methane is expected to be rather small and fairly insensitive to the sign of the ion charge. To illustrate these ideas, we compute the solvation-free energy of a sodiumlike ion from simulations based on a finite spherical drop of methane. As shown in Table III the computed free energy difference between a positively and negatively charged sodiumlike ion is approximately zero. This is in stark contrast to the 10.0 kcal/mol energy that is associated with transferring a $+1e$ versus a $-1e$ test charge across a potential the size of the liquid methane-vacuum interface potential. The discrepancy in these values simply reflects the inclusion of both the macroscopic liquid-vacuum and microscopic solute-vacuum interfaces in the solvation-free energy simulation. Also included in Table III, is the difference in solvation-free energy between the positive and negative sodiumlike ions from a simulation that is conducted in periodic boundary conditions. The computed difference in free energy, of approximately −10 kcal/mol, is an artifact that reflects the absence of any macroscopic

liquid-vacuum interface in this system. Applying a correction for this term gives the correct, nearly zero free energy difference.

Unlike the nonpolar methane solvent, the potential at the center of a LJ sphere solvated in liquid water (ϕ_{micro}) depends nontrivially on the size of the sphere. For a LJ sphere the size of a sodiumlike ion, $\phi_{\text{micro}} \approx -0.9\phi_{l\to v}$.[39] The rather small difference between these potentials is a consequence of the differing anisotropic contributions to the interface potential from the orientation of molecular dipoles at the respective solute-solvent and solvent-vacuum interfaces. As the solute grows in size it begins to take on the physical characteristics of the macroscopic solvent-vacuum interface and $\phi_{\text{micro}} \to -\phi_{l\to v}$.[39] Resolving this difference between ϕ_{micro} and $\phi_{l\to v}$ in the small solute limit is beyond the scope of the present analysis.

V. CONCLUSIONS

Atomic level simulations of both polar and nonpolar systems consistently predict a significant interfacial potential between a gaseous and condensed phase. This observation cannot be explained by the orientational ordering of molecules alone. To address the missing conceptual element in the analysis of such potentials we construct a simple model for the interface potential. The model considers molecules to be isotropically oriented, averaging away the intermolecule complexity of the system.

The model captures, with quantitative precision, the surprisingly large IP that is calculated from a molecular simulation of a vacuum-hydrocarbon interface. Applying the model to the vacuum-methane system, the model predicts an interface potential of −220 mV, in agreement with a MD simulation. For polar molecules, such as water, a nontrivial contribution to the interface potential from particular orientational ordering of molecules at the interface is also to be expected. For such systems the model serves as a zeroth-order approximation, where contributions from the molecular dipoles are canceled due to orientational averaging. Nevertheless, the model qualitatively captures the sign and magnitude of the interface potential calculated from a MD simulation of the vacuum-water interface system, which is roughly −500 mV.

That such a model, based solely on the properties of a single molecule, can capture the interface potential of an atomic level detailed interface system is surprising, although it is important to place the isotropic contribution to the interface potential in a proper physical context. The relevant observable for the solvation of a charged species include not only the macroscopic potential from the vacuum-solvent interface but also a compensatory interface potential at the solute-solvent interface. For a purely isotropic model these contributions cancel and solute solvation will be independent of the interface potential. As a practical consideration, the calculation of solvation free energies from purely bulk liquid simulations, which only include the microscopic solute-solvent interface potential, should therefore take care to include a model specific contribution from the vacuum-solvent interface potential.

ACKNOWLEDGMENTS

Financial support to B.R. was acknowledged from the NIH (No. GM 072558) and NSF (No. MCB-0110847). We would like to thank Philippe Hünenberger, Olaf Andersen and Alex MacKerell, Jr. for helpful discussions.

APPENDIX

The probability of finding charge in an infinitesimal slice δz at z for a single molecule centered at the origin is

$$P_i(z, z_c = 0)\,\delta z = \frac{\int_r^{r+\delta r}\int_0^{2\pi}\int_0^{\pi} e^{-(r-r_i)^2/2\sigma_i^2} r^2 \sin(\phi)\, d\phi\, d\theta\, dr}{C_i},$$

The normalization factors are

$$C_i = \int_0^{\infty}\int_0^{2\pi}\int_0^{\pi} e^{-(r-r_i)^2/2\sigma_i^2} r^2 \sin(\phi)\, d\phi\, d\theta\, dr,$$

$$= 2\pi\left(2\sigma_i^2 r_i e^{-r_i^2/2\sigma_i^2} + \sqrt{2\pi}\sigma_i(r_i^2+\sigma_i^2)\left(1+\operatorname{erf}\left(r_i/\sqrt{2}\sigma_i\right)\right)\right).$$

For $z > 0$,

$$P_i(z, z_c = 0)\,\delta z = 2\pi(2^{3/2}\sigma_i^3) \times \frac{\int_{|z'|/\cos(\phi)}^{(|z'|+\delta z')/\cos(\phi)}\int_0^{\pi/2} e^{-(r'-r_i')^2} r'^2 \sin(\phi)\, d\phi\, dr'}{C_i},$$

where $r' = r/\sqrt{2}\sigma_i$, $z' = z/\sqrt{2}\sigma_i$, and $r_i' = r_i/\sqrt{2}\sigma_i$. Evaluating the following integral,

$$A = \int_{|z|/\cos(\phi)}^{(|z|+\delta z)/\cos(\phi)}\int_0^{\pi/2} e^{-(r-r_i)^2} r^2 \sin(\phi)\, d\phi\, dr,$$

$$= \int_0^{\pi/2} \delta z |z|^2 e^{-(|z|/\cos(\phi)-r_i)^2} \frac{\sin(\phi)}{\cos(\phi)^3} d\phi,$$

$$= \frac{\delta z}{2}\left(e^{-(|z|-r_i)^2} + \sqrt{\pi} r_i \left(1+\operatorname{erf}(r_i - |z|)\right)\right),$$

and substituting A back into P_i, we get,

$$P_i(z, z_c) = \frac{2\pi\left(\sigma_i^2 e^{-(r_i-|z-z_c|)^2/2\sigma_i^2} + \sigma_i r_i \sqrt{\frac{\pi}{2}}\left(1+\operatorname{erf}\left(\frac{r_i-|z-z_c|)}{\sqrt{2}\sigma_i}\right)\right)\right)}{C_i},$$

In the limit $\sigma_i \to 0$ the probability reduces to a Heavyside function,

$$P_i(z, z_c) = \frac{\Theta(r_i - |z - z_c|)}{2r_i}.$$

[1] J. Cladera and P. O'Shea, Biophys. J. **74**, 2434 (1998).
[2] T. I. Rokitskaya, Y. N. Antonenko, and E. A. Kotova, Biophys. J. **73**, 850 (1997).
[3] N. Thompson, G. Thompson, C. D. Cole, M. Cotten, T. A. Cross, and D. D. Busath, Biophys. J. **81**, 1245 (2001).
[4] B. Maggio, J. Lipid Res. **40**, 930 (1999).

[5] O. S. Ostroumova, V. V. Malev, and A. N. Bessonov, Langmuir **24**, 2987 (2008).
[6] Y. A. Liberman and V. P. Topaly, Biofizika **14**, 452 (1969).
[7] D. A. Haydon and V. B. Myers, Biochim. Biophys. Acta **307**, 429 (1973).
[8] S. B. Hladky and D. A. Haydon, Biochim. Biophys. Acta **348**, 464 (1973).
[9] M. Paluch, Adv. Colloid Interface Sci. **84**, 27 (2000).
[10] I. Benjamin, Annu. Rev. Phys. Chem. **48**, 407 (1997).
[11] B. C. Garrett, Science **303**, 1146 (2004).
[12] J. H. Seinfeld, Science **288**, 285 (2000).
[13] P. Jungwirth and D. J. Tobias, Chem. Rev. (Washington, D.C.) **106**, 1259 (2006).
[14] G. Lamoureux and B. Roux, J. Phys. Chem. B **110**, 3308 (2006).
[15] Y. N. Vorobjev and J. Hermans, J. Phys. Chem. B **103**, 10234 (1999).
[16] C. D. Wick, L. X. Dang, and P. Jungwirth, J. Chem. Phys. **125**, 024706 (2006).
[17] G. Lamoureux, A. D. MacKerell, Jr., and B. Roux, J. Chem. Phys. **119**, 5185 (2003).
[18] M. Matsumoto and Y. Kataoka, J. Chem. Phys. **88**, 3233 (1988).
[19] M. A. Wilson, A. Pohorille, and L. R. Pratt, J. Chem. Phys. **90**, 5211 (1989).
[20] S. Patel and C. L. Brooks III, J. Chem. Phys. **124**, 204706 (2006).
[21] G. Hummer, L. R. Pratt, A. E. Garcia, S. Garde, B. J. Berne, and S. W. Rick, J. Phys. Chem. B **102**, 3841 (1998).
[22] H. S. Ashbaugh, Mol. Phys. **97**, 433 (1999).
[23] A. D. MacKerell, Jr., B. Brooks, C. L. Brooks III, L. Nilsson, B. Roux, Y. Won, and M. Karplus, in *Encyclopedia of Computational Chemistry* (Wiley, Chichester, 1998), Vol. 1.
[24] M. P. Allen and D. J. Tildesley, *Computer Simulation of Liquids* (Oxford University Press, New York, 1987).
[25] G. J. Martyna, M. L. Klein, and M. Tuckerman, J. Chem. Phys. **97**, 2635 (1992).
[26] G. J. Martyna, D. J. Tobias, and M. L. Klein, J. Chem. Phys. **101**, 4177 (1994).
[27] U. Essmann, L. Perera, M. L. Berkowitz, T. Darden, H. Lee, and L. G. Pedersen, J. Chem. Phys. **103**, 8577 (1995).
[28] H. C. Andersen, J. Comput. Phys. **52**, 24 (1983).
[29] G. J. Martyna, M. E. Tuckerman, D. J. Tobias, and M. L. Klein, Mol. Phys. **87**, 1117 (1996).
[30] W. L. Jorgensen, J. Chandrasekhar, J. D. Madura, R. W. Impey, and M. L. Klein, J. Chem. Phys. **79**, 926 (1983).
[31] A. D. MacKerell, Jr., D. Bashford, M. Bellott, R. L. Dunbrack, Jr., J. D. Evanseck, M. J. Field, S. Fisher, J. Gao, H. Guo, S. Ha, D. Joseph-McCarthy, L. Kuchnir, K. Kuczera, F. T. K. Lau, C. Mattos, S. Michnick, T. Ngo, D. T. Nguyen, B. Prodhorn, W. E. Reiher III, B. Roux, M. Schlenkrich, J. C. Smith, R. Stote, J. Straub, M. Watanabe, D. Wirkiewicz-Kuczera, D. Yin, and M. Karplus, J. Phys. Chem. B **102**, 3586 (1998).
[32] P. Liu, E. Harder, and B. J. Berne, J. Phys. Chem. B **109**, 2949 (2005).
[33] Y. Deng and B. Roux, J. Phys. Chem. B **108**, 16567 (2004).
[34] J. W. Cahn and J. E. Hilliard, J. Chem. Phys. **28**, 258 (1958).
[35] J. D. Jackson, *Classical Electrodynamics*, 2nd ed. (Wiley, New York, 1975).
[36] M. C. Goh, J. M. Hicks, K. Kemnitz, G. R. Pinto, T. F. Heinz, K. B. Eisenthal, and K. Bhattacharyya, J. Phys. Chem. **92**, 5074 (1988).
[37] M. A. Wilson, A. Pohorille, and L. R. Pratt, J. Chem. Phys. **88**, 3281 (1988).
[38] M. Born, Z. Phys. **1**, 45 (1920).
[39] S. Rajamani, T. Ghosh, and S. Garde, J. Chem. Phys. **120**, 4457 (2004).
[40] D. Cerutti, N. Baker, and J. McCammon, J. Chem. Phys. **127**, 155101 (2007).
[41] H. S. Ashbaugh, J. Phys. Chem. B **104**, 7235 (2000).
[42] M. A. Kastenholz and P. H. Hünenberger, J. Chem. Phys. **124**, 124106 (2006).
[43] B. A. Pethica, Phys. Chem. Chem. Phys. **9**, 6253 (2007).